HHS Public Access

Author manuscript

Neuroimage. Author manuscript; available in PMC 2017 June 01.

Published in final edited form as:

Neuroimage. 2016 June ; 133: 129–143. doi:10.1016/j.neuroimage.2016.03.012.

Bi-directional changes in fractional anisotropy after experiment TBI: disorganization and reorganization?

N. G. Harris[1], **D.R. Verley**[1], **B.A. Gutman**[2], and **R.L. Sutton**[1]

[1]UCLA Brain injury Research Center, Department of Neurosurgery, University of California, Los Angeles, USA

[2]Imaging Genetics Center, Institute for Neuroimaging and Informatics, Department of Neurology, Keck/USC School of Medicine, University of Southern California, Los Angeles, CA, USA

Abstract

The current dogma to explain the extent of injury related changes following rodent controlled cortical impact (CCI) injury is a focal injury with limited axonal pathology. However, there is in fact good, published histologic evidence to suggest that axonal injury is far more widespread in this model than generally thought. One possibility that might help to explain this is the often-used region-of-interest data analysis approach taken by experimental traumatic brain injury (TBI) diffusion tensor imaging (DTI) or histologic studies that might miss more widespread damage, when compared to the whole brain, statistically robust method of tract based analysis used more routinely in clinical research. To determine the extent of DTI changes in this model, we acquired *in vivo* DTI data before and at 1 and 4 weeks after CCI injury in 17 adult, male rats and analyzed parametric maps of fractional anisotropy (FA), axial, radial and mean diffusivity (AD, RD, MD), tensor mode (MO), and fiber tract density (FTD) using tract based spatial statistics. Contusion volume was used as a surrogate marker of injury severity and as a covariate for investigating severity dependence of the data. Mean fiber tract length was also computed from seeds in the cortical spinal tract regions. In parallel experiments (n=3–5/group) we investigated corpus callosum neurofilaments and demyelination using immunohistochemistry (IHC) at 3 days and 6 weeks, callosal tract patency using dual-label retrograde tract-tracing at 5 weeks, and the contribution of gliosis to DTI parameter maps using GFAP IHC at 4 weeks post-injury. The data show widespread ipsilateral regions of significantly reduced FA at 1 week post-injury, driven by temporally changing values of AD, RD and MD that persist to 4 weeks. Demyelination, retrograde label tract loss, and reductions in MO (tract degeneration) and FTD were shown to underpin these data. Significant FA increases occurred in subcortical and corticospinal tract regions that were spatially distinct from regions of FA decrease, grossly affected gliotic areas and from MO changes. However, there was good spatial correspondence between regions of increased FA and areas of increased FTD and mean fiber length. We discuss these widespread changes in DTI parameters in

Address for Correspondence: Neil G. Harris, Ph.D, Department of Neurosurgery, David Geffen School of Medicine at UCLA, 300 Stein Plaza, Ste 535, Box 956901, Los Angeles, CA 90095-7039, Telephone: +1-(310)-206.5691, FAX: +1801672.1018, ; Email: ngharris@mednet.ucla.edu

terms of axonal degeneration and potential reorganization, with reference to a resting state fMRI companion paper (Harris et al, 2016, Exp. Neurol.227:124–138) that demonstrated altered functional connectivity data acquired from the same rats used in this study.

Graphical Abstract

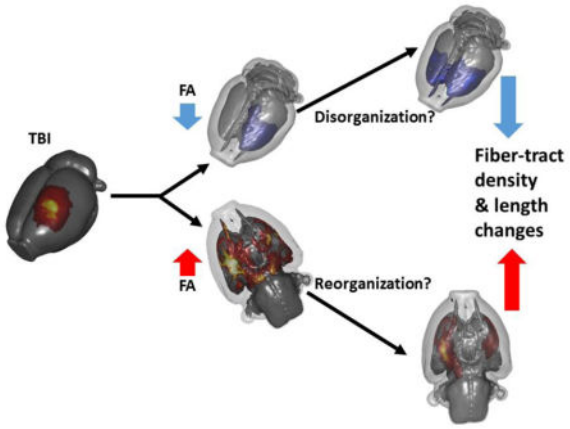

Keywords

plasticity; structural reorganization; connectivity; controlled cortical impact; rat; imaging; MRI

Introduction

Over the past two decades or more, diffusion tensor imaging (DTI) has gained wide acceptance for delineating white matter pathology after traumatic brain injury (TBI). It is being used increasingly for clinical research-based detection of abnormalities in mild to severe TBI patients (Rutgers et al., 2008) including blast injury (Mac Donald et al., 2011). The commonly used diffusion indices derived from the tensor model fit of DTI data provide insight into the directionality and magnitude of the movement of protons in the presence of diffusion-sensitizing gradients. A full understanding of the tissue pathology changes that result in alteration in diffusion characteristics is an ongoing process in many CNS diseases states, for example multiple sclerosis (Budde et al., 2009; Chiang et al., 2014; Song et al., 2002) as well as TBI (Budde et al., 2011; Laitinen et al., 2015; 2010; MacDonald et al., 2007). Given the potential importance of DTI metrics as biomarkers of disease stage, severity, and outcome, a thorough study relating pathogenesis and imaging parameters is required to promote their understanding and wider use. In addition to using fractional anisotropy (FA), the degree of unidirectional movement of protons within a gradient, as an indicator of axonal integrity after TBI, it is also used to delineate fiber tract pathways using one of the many tracking algorithms available. As a result, it is important to determine when DTI metrics become less affected by altered tissue integrity post-injury, for example vasogenic edema or increased cell density (Chiang et al., 2014). This should increase confidence that FA and tractography data used in the computation of structural connectomes can be relied upon to reflect solely a measure of patent fiber tract pathways and network changes, and is free from confounds related to continuing disease pathology.

While evidence from adult rodent experimental TBI studies has shown that DTI parameters closely relate to axonal injury within 24hrs of a cortical contusion in mice (MacDonald et al., 2007), this relationship has been found to be substantially influenced by gliosis in grey matter at 2 months post-injury in a rat contusion model (Budde et al., 2011). These and other studies in rodent TBI models (Laitinen et al., 2015; Zhuo et al., 2012) indicate that the interpretation of pathology corresponding to DTI parameter changes is not straightforward, and that further study is required. Perhaps even more controversial in the TBI field is the finding and interpretation of an increase of FA after injury. There are several clinical investigations that report this and discuss the implications in terms of pathology, injury severity, and functional outcome within regions of both white and grey matter (Cubon et al., 2011; Ling et al., 2012; Lipton et al., 2012; Mayer et al., 2015; Messé et al., 2010). The majority of studies using *in vivo* DTI in adult rodent TBI models report decrease in white matter FA in association with axonal injury (Laitinen et al., 2015; Long et al., 2015; MacDonald et al., 2007; Sierra et al., 2011; Xu et al., 2011). Most experimental DTI studies use a region-of-interest (ROI)-based approach to data analyses that might miss some important changes related to more subtle injury pathology. In fact, of the few existing studies using whole brain, voxel-based analysis of DTI parameters, an increase rather than a decrease in thalamic FA was reported at 30 days after blast injury in the mouse (Rubovitch et al., 2011) as well as in the ipsilateral barrel cortex at 12 weeks after lateral fluid percussion injury (Johnstone et al., 2015). Therefore, it remains a possibility that a more statistically robust, whole brain analysis of white matter tracts, will provide a greater indication of pathology after TBI in rodent models. As whole brain analysis is used routinely in clinical studies, such a study may also uncover greater similarities to clinical data. In the controlled cortical impact injury (CCI) model of TBI, contrary to current dogma on the focal nature of the injury, there is in fact widespread axonal degeneration both bilaterally as well as caudally in the forebrain after CCI injury, as indicated by silver staining data (Hall et al., 2008, 2005; Matthews et al., 1998). We hypothesize that a whole brain approach to rodent DTI analysis would yield a better approximation to the total amount of axonal damage present after CCI injury as reflected in those studies.

Based on these prior data and preliminary work using DTI in this model (Harris et al., 2009), we acquired *in vivo* DTI data before and at 1 and 4 weeks after injury using the CCI injury model in adult rats, in an effort to understand the temporal and spatial nature of FA changes after TBI. We hypothesized that a white matter tract-based spatial statistical approach to rodent DTI analysis would provide a more widespread delineation of axonal pathology after rodent contusion injury more comparable to prior silver staining studies. We also acquired dual-label, retrograde dye-injection tract-tracing data together with immunohistochemistry data of myelination and gliosis status to provide further verification of the DTI changes. We discuss these data in terms of the many known confounds that underlie the DTI indices, and with particular reference to a resting state fMRI companion paper (Harris et al, 2016) that demonstrated significantly altered functional connectivity from data that we acquired from the same rats and similar time-points used in this study.

Methods

Experiment Protocol

DTI data were acquired on a 7 Tesla Bruker MRI from adult rats (n=17) under isofluorane sedation before CCI injury and at 7 and 28 days after brain injury. Additional groups of rats were used for dual-label tract-tracing at 35 days post-injury (n=3/group) and for immunohistology at 3, 28, and 42 days post-injury (n=3–5/group).

Brain Injury

All study protocols were approved by the University of California Los Angeles Chancellor's AnimalResearch Committee and adhered to the Public Health Service Policy on Humane Care and Use of Laboratory Animals. The method for induction of moderate CCI injury was performed in the manner similar to previously described.([Chen et al., 2003](), [2004](); [Chen et al., 2002](); [Harris et al., 2012](), [2010a](), [2010b]()) Briefly, male, Sprague-Dawley rats (220–250g body weight) were anaesthetised with 2% isofluorane vaporized in O_2 flowing at 0.6 L/min and placed on a homeostatic temperature-controlled blanket while maintained in a stereotactic frame. CCI injury was produced using a 4mm diameter impactor tip that was advanced through a 5mm craniotomy (centered at 0.0mm Bregma and 3mm left-lateral to the sagittal suture) onto the brain using a 20psi pressure pulse, and to a deformation depth of 2 mm below the dura. The craniotomy site was covered with a non-toxic, rapid curing silicone elastomer (WP Instruments, USA) and the wound was closed with sutures.

MRI Acquisition

Rats were briefly anesthetized with 4% isofluorane in oxygen flowing at 0.6 l/min and then transferred to a purpose-built cradle and secured using three-point immobilization of the head with two ear bars and a tooth bar. Resting state functional MRI (rsFMRI) data were then acquired from all rats under medetomidine sedation for 45 minutes prior to resuming isoflurane sedation at 1.2 – 1.5% for the remainder of the imaging session to collect the diffusion imaging data reported in this manuscript. This rsFMRI data and the details of the medetomidine sedation has been published ([Harris et al, 2016]()). The rat cradle was placed in the center of a 7 Tesla spectrometer (Oxford Instr, Carteret, NJ, USA) driven by a Bruker console running Paravision 5.1 (Billerica, MA USA). Respiration was monitored remotely and temperature was homeothermically-controlled by forced air (SA11 Instr, Inc, USA). The S116 Bruker gradients (400mT/m) were used in combination with a birdcage transmit and an actively decoupled, receive-only surface coil to acquire the data. Following a multi-slice, gradient-echo pilot scan to optimize positioning within the magnet, localized shimming was performed on the head to improve B0 homogeneity. A standard, 4-shot, spin echo, echo planar imaging sequence (6250/32ms repetition and echo time, respectively) was used to acquire diffusion-weighted images with directionally-encoded gradients applied along 30 different, even-spaced directions and with a b value of 1000 s/mm^2, using Δ=20ms and δ=3ms. Five additional images were acquired with a b value of 0 s/mm^2. All images were acquired with a 128-read and 128-phase-encoding matrix (X,Y direction respectively) within a 35mm^2 field-of-view and 25 × 0.75mm contiguous, coronal slices, resulting in an in-plane resolution of 273 × 273μm and a 750μm slice thickness. Anatomical, T2-weighted, rapid-relaxation-with-enhancement (RARE) data were acquired with 50×0.5mm slices, 128-read

x128-phase-encoding matrix within a 35×35mm field-of-view, a TR/TE 5000/60ms repetition and echo time, respectively, a RARE factor of 8 and 2 averages.

Retrograde Tract Tracing and Immunostaining

Additional injured (post-injury day 28) and naïve control rats that were not imaged in this study (n=3/group) were used for tract tracing. The retrograde tract tracers Fluorogold (FG, 5% solution Sigma-Alrich, USA) in artificial cerebrospinal fluid, (aCSF, Harvard Apparatus, USA) and cholera toxin B (CTB, 1% solution in aCSF, List Biological Labs, Campbell, CA, USA) were injected into layer V of the cortex (1.5mm below dura) lateral (0mm, Bregma, 5mm lateral) and medial (0mm Bregma, 0.5mm lateral) to the contusion, respectively, using 1.5μl of each marker at an injection rate of 0.1 μl/min with a Hamilton syringe (Hamilton, Reno, USA) connected to a 33G needle and a microinjection pump (Stoelting, Wood Dale, IL). Following injection, the needle was left in place for 10 minutes to prevent backflow of the tracer through the needle tract. After 7 days (post-injury day 35) brains were fixed by transcardial perfusion-fixation with 0.1M phosphate-buffered saline and 4% paraformaldehyde in phosphate buffer, excised from the skull, cryo-protected in 20% sucrose solution until sunk, and coronally sectioned at 50μm using a cryostat (Leica, USA). For each brain, two anterio-posterior sets of sections, 600μm apart, were processed for standard free-floating, single label immunohistochemistry for each tracer. Briefly, after quenching for 1hr (methanol and hydrogen peroxide), washing in tris-buffered saline (TBS), and blocking for 2hrs (3% normal goat serum [NGS] and 0.25% triton-x in TBS) sections were exposed to the primary antibodies (rabbit polyclonal, anti-fluorogold, 1:500 [#AB153, Millipore, USA] or goat anti-cholera toxin B, 1:500 [List Biological Labs, Campbell, CA, USA]) in 1% NGS in TBS overnight. After washing and exposure to a secondary biotinylated antibody, 1:500 (Invitrogen, USA), binding was visualized using the avidin-biotin reaction with diaminodenzidine (Vector Labs, Burlingame, CA, USA). Sections were mounted on gelatin coated slides and dehydrated and cover-slipped. For visual clarity, stained cells on 1 section per brain at Bregma 0mm were roughly mapped out onto an atlas and overlaid to show tracer overlap. Unbiased stereologic analysis was performed to estimate the total number of FG and CTB-labelled cell bodies in the contralateral cortex as an indicator of reduced callosal connectivity using a Leica upright microscope (DMR, Leica, USA) interfaced to a stereology system (MicroBrightfield, Williston, VT, USA). The optical fractionator method was implemented using Stereoinvestigator software (MicroBrightfield, Williston, VT, USA) on 3 sections/brain, spaced 600μm apart around Bregma. Contours were drawn to encompass the grey matter from the midline to a line running perpendicular to the rhinal fissure. Group differences in the resulting estimated cell counts were assessed using a one-way analysis of variance.

Additional injured and craniotomy-sham control rats that were not imaged in this study were used to assess neurofilaments and myelin at 3 days and 6 weeks after injury (n=5/group). Tissue was processed and sectioned as described above and exposed to primary antibodies raised against axonal neurofilament 160kD (1:75, #AB7794, Abcam, USA) and myelin basic protein (1:200, #A0623, Dako, USA), respectively. Binding was visualized using primary-host specific secondary antibodies conjugated to the fluorophores: alexa-488 and alexa-555 (1.25 μg/mL in TBS for 60 minutes; Molecular Probes/Invitrogen, Carlsbad, CA). Sections

were mounted on slides and cover-slipped with anti-bleaching medium (Vector Laboratories, USA). Double-labeled sections (5/brain) were imaged by confocal microscopy (LSM Pascal System; Zeiss, Thornwood, NY) in single-channel acquisition mode to prevent crosstalk and with fluorophore-appropriate laser excitation and filter sets configured for optimal emission. Montage (X–Y) data were acquired with a 12-μm optical section thickness at 4×0 magnification over 4 to 8 fields of view in automatic mode. Sections representative of these data are shown in our results.

A final set of injured and craniotomy-sham control rats that were not imaged in this study were used to assess gliosis at 4 weeks post-injury (n=3/group), as done previously (Chen et al., 2003). Tissue was processed and sectioned as above and exposed to primary antibody against GFAP (1:500, #Z0334, Dako, USA) and visualized with the avidin-biotin reaction using diaminodenzidine as before. Representative images were captured using an upright M2 Zeiss microscope using a x10 objective and stitched using Axiovision (Zeiss, USA).

MRI Data Analysis and Statistics

Data were Fourier transformed and converted to compressed NIFTI format, corrected for eddy current distortions using eddy correct (FSL, FMRIB Software Library, University of Oxford, UK) after which DTIFIT (FSL, FMRIB, Oxford UK) was used with the gradient vectors and diffusion weighting b values to fit the tensor model at each voxel in order to generate scalar maps of fractional anisotropy (FA), three eigenvalue maps (lambda 1–3) of the three principal eigenvectors, and mean diffusivity (MD), the average eigenvalue. Lambda 1 is referred to here as axial diffusivity (AD) and the average of lambda 2 and 3 was calculated voxel-wise for each brain and is referred to here as radial diffusivity (RD). Tensor shape was also fitted and parameterized between −1 and 1 as the mode of the tensor (MO, see results section) (Ennis and Kindlmann, 2006; Kindlmann et al., 2007). Data were analyzed using the tract based spatial statistics (TBSS) pipeline implemented by FSL, FMRIB (Smith et al., 2006) and adapted for the rat. FA images were used to coregister the data to a common rat template space (Valdés-Hernández et al., 2011) outside of the TBSS pipeline using an implementation of FSL flirt(Jenkinson and Smith, 2001; Jenkinson et al., 2002) adapted for the rat (Crum et al., 2013). The axonal skeleton mask was generated using an FA threshold of 0.26 and was projected onto the data and tested for voxel-wise group FA differences by nonparametric permutation inference using Randomise with the general linear model (Winkler et al., 2014) using an unpaired t-test against pre-injury data to determine regions where FA was significantly higher or lower. Except where stipulated, cluster-based thresholding was performed, corrected for multiple comparisons by using the null distribution of the maximum cluster size (c=1.7) and using a family-wise error rate of $P<0.05$. We used a variance smoothing of 0.5mm and 5000 permutations to generate a null distribution of interest. Contusion volume at 28 days post-injury was used as a surrogate marker of injury severity, and was entered as a covariate within the statistical design. This was estimated from the T2-weighted, anatomical data by summing the volume of the ipsilateral cortical voxels with a greyscale intensity greater than 2 standard deviations above the mean intensity of the cortical grey matter of the contralateral hemisphere immediately opposite the primary injury site. The scalar maps of AD, RD, MD and MO were warped into template space using the matrix transformations obtained by registering FA images, and

were then tested for group differences as described above. Crossing fibers were modelled in three rats before and after injury. BEDPOSTX (Bayesian estimation of diffusion parameters obtained using sampling techniques) was used to model 2 fibers per voxel using default running parameters (Behrens et al., 2007, 2003).

Fiber tract density (FTD) data were generated from pre-injury and 28 day post-injury data by deterministic fiber-tracking using Diffusion Toolkit and Trackvis software (Ruopeng Wang, Van J. Wedeen, TrackVis.org, Martinos Center for Biomedical Imaging, Massachusetts General Hospital, MA). The FACT algorithm was used to fiber track the data (Mori et al., 1999) in native space and with a step length of 0.1, a maximum turning angle of 50° and an FA cutoff of 0.2. A whole brain mask generated by the BET algorithm (Smith, 2002) was used to seed and to constrain the tracks at the brain surface. Track data was then used to generate FTD maps where the voxel value reflects the numbers of fibers that contact that voxel. These scalar maps were then warped into template space using the image matrix transformations obtained with the FA data, and were then tested for group differences as described above.

Given the current interest in imaging biomarkers of disease, we also determined the regions of injured brain where the diffusion scalars were associated with the degree of injury severity. This was implemented in the same way as before using Randomize (Winkler et al., 2014) to interrogate the data for significant correlations with injury severity. In addition, all voxels showing significant correlation were entered into a univariate linear regression of DTI metric by injury severity to confirm the correlation. Tract length data were generated from each tractography dataset by warping the group level map of significant FTD into the native space of each brain map for use as a seed region. Tract length data were also generated from internal capsule regions that were extracted from a parcellated atlas of the rat brain and warped to each native space. The atlas was constructed by co-registering a parcellated cortical atlas (Valdés-Hernández et al., 2011) with subcortical structures (https://www.nitrc.org/projects/dti_rat_atlas/) together with numerous other structures from our in-house atlas which itself was manually constructed in 3-dimensions using Itksnap (Yushkevich et al., 2006) with reference to a 2-dimensional atlas (Paxinos and Watson, 1997). The final atlas consisted of 148 individual, parcellated regions.

Results

Given the marked bi-directionality of the FA data, the following results section is organized by first reporting regions of decreased FA at both 1 and 4 weeks post-injury, followed by increased FA at these same time time-points.

One week post-trauma is marked by reductions in white matter FA underpinned by increased RD

Data at 7 days post-injury showed marked, ipsilateral reductions in FA, extending from the cingulum to the external capsule, regions that underlie the motor and sensory cortical regions anteriorly from Bregma +2.2mm to the posterior, midline retrosplenial cortex around Bregma −4.3 (Fig. 1A–C, $P<0.05$, corrected). No significant subcortical FA changes were found. The major diffusion eigenvalues driving the white matter FA reduction were $\lambda 2$ and

λ3 or radial diffusivity (RD) - diffusion perpendicular to the major movement of water molecules along the axon fibers. This was significantly increased from pre-injury within this area of reduced diffusion anisotropy (Fig. 1E), while λ1 - axial diffusivity (AD, Fig. 1D), and the mean of the major eigenvalues - mean diffusivity (MD, Fig. 1F), were unchanged. When the diffusion scalars were assessed globally over the brain unconstrained by FA changes, we found no brain regions significantly affected by injury that survived correction for multiple voxel comparison, except for contralateral reductions in RD within the caudate putamen and internal capsule (Fig. 1G).

There was considerable variation in injury diffusivity at 7 days compared to pre-injury (Fig. 1C–F), and therefore we examined whether injury severity was an underlying cause. Previous work in this model has shown contusion volume to be consistent within-group early after injury, with greater variation at 4 weeks (Chen et al., 2003), and this is presumably due to different rates of atrophy that occur due to even minor variations in the location and severity of the initial injury. In order to obtain a more accurate measure of injury severity in the current work, we measured contusion volume at 4 weeks post-injury for input as a covariate for the TBSS analysis. The data showed some degree of variation among the group as indicated by contusion volume projected onto the cortical surface (Fig. 3A). We tested whether the degree of injury was a significant driver of the diffusion scalar changes, with the hypothesis that greater injury would lead to a further departure from pre-injury values for each of the parameters measured. This was indeed the case for FA values (Fig. 2A, B) which was negatively correlated to severity ($r^2=-0.78$, $P<0.001$, Fig. 2C) within the same ipsilateral white matter regions that showed significant reductions in FA (Fig. 2A–B). Surprisingly AD, RD, and MD did not correlate with injury within the same regions at 7 days; injury-associated reductions in RD and MD were found only in the contralateral internal capsule and medial forebrain bundle (Fig. 2D–F, $r^2=-0.50$, $P=0.005$ and Fig. 2G–I, $r^2=-0.52$, $P=0.004$, respectively) but AD was not significant.

Four weeks post-trauma is marked by persistent reductions in white matter FA and increases in AD, RD and MD

The DTI data at 28 days post-injury displayed a similar trend to 7 days, with persistent reductions in magnitude of FA within the ipsilateral corpus callosum, with additional significant reductions in the hippocampal fimbria (Fig. 3B,C). However unlike at 7 days, FA reductions were underpinned by significant increases in AD and RD, as well as MD within this region when assessed within the same region, rather than simply RD alone (Fig. 3D, E, F, respectively). However, when these parameters were assessed globally over the brain unconstrained by reductions in FA, we found widespread increases in all three diffusion indices (Fig. 3G, H, I, respectively). The affected region far exceeded the area of reduced FA, as indicated by widespread increases within rostral-caudal and contralateral regions of the corpus callosum, as well as in bilateral thalamic regions. These more extensive changes in diffusivity among the major tensor vectors implies that the ratio of eigenvalues that contribute to changes in FA might be far less sensitive to pathology than individual diffusion vectors alone. This would explain the absence of a significant decrease in FA within the ipsilateral cingulum at 28 days when one existed at 7 days (Fig. 3B vs Fig. 1A,B) because there was increased diffusion in all directions in this region at 28 days resulting in no net

change in FA, while only RD was significantly altered at 7 days. These data suggest that parallel changes in AD and RD in the absence of FA changes, for example in contralateral corpus callosum and thalamus, only occur in less severely injured tissue (Fig. 3G,H versus Fig. 3B). Meanwhile, in white matter regions that are more severely injured immediately under the contusion (Fig. 3B), FA is reduced along with AD and RD (Fig. 3G,H)

Cellular basis for diffusivity changes

Tissue immunohistochemistry for neurofilaments and myelin basic protein performed at similar acute and chronic post-injury times as the DTI data show that the early reduction in FA and increased RD in corpus callosum is consistent with cytoskeletal breakdown and demyelination (Fig. 4A–D). The lack of significant change in AD at acute post-injury times likely reflects the complex pathology occurring at this time, as indicated by the grossly varying, within-group values of AD (Fig. 2D). Further loss of neurofilaments at more chronic times together with clearance of myelin debris (Fig. 3E) is consistent with continued reduction in FA and large increases in all diffusion vectors at this post-injury time (Fig. 3). The much less affected white matter pathology in regions at the medial and lateral edges of the region of reduced FA (Fig. 4A, regions 1 and 4) suggest that even minor disturbances in myelin and axonal structure beyond the relatively gross cellular-level resolution shown here result in diffusivity changes.

Given the on-going interest in imaging parameters as disease biomarkers, the finding of marked variation in diffusion parameters at 4 weeks post-injury (Fig. 3C–F), and the acute post-injury association of injury severity with diffusivity (Fig. 2), we investigated whether injury severity continues to drive the diffusion scalar changes at a more chronic time post-injury. We found that similar to 7 days, FA was negatively associated with increasing injury (Fig. 5A–C), however this association was present bilaterally rather than being constrained to the ipsilateral hemisphere as it was acutely (Fig. 2A–C). This presumably reflects on-going Wallerian degeneration between the hemispheres. However unlike at 7 days, AD, RD and RD were positively, rather than negatively correlated to injury severity at 28 days, and within ipsilateral white matter regions (Fig. 5D–L) rather than contralateral subcortical regions as they were acutely (Fig. 2D,E,G,H). Surprisingly these correlations did not follow the bilateral white matter association of FA with injury severity (Fig. 5A,B), indicating the complexity of interpreting this ratio metric.

To provide an independent measure of how far the axonal damage extended from the injury site, we injected the retrograde axon tracer fluorogold (FG) in ipsilateral cortex and lateral to the contusion in 3 moderately injured rats at 35 days post-injury and in 3 naïve rats (Fig. 6A,B) and confirmed a ~50% reduction in the number of FG-labelled cells in the contralateral grey matter as an indication of axon injury at and beyond the primary injury site (Fig. 6C,D, $P<0.05$). In the same animals, we also injected the retrograde marker cholera toxin B (CTB) in ipsilateral cortex but medial to the injury site into the spared M1/M2 cortical region (Fig. 6E, F) that overlies white matter that is less affected by axon injury (Fig. 4E, region 1). The number of CTB-labelled cells in the contralateral cortex was again reduced by ~50% compared to naïve controls (Fig. 6G, H, $P<0.05$). Similar results for the lateral and medial tracer injections suggests that white matter damage extends into the

contralateral hemisphere by day 28, proving a morphological basis for the bilateral correlation of FA with injury severity in this region (Fig. 5A).

FA increases occur in subcortical regions at both 1 and 4 weeks post-injury

A number of clinical publications have shown there to be increases in FA after injury (Bazarian et al., 2007; Henry et al., 2011; Mayer et al., 2010; Wilde et al., 2008) and therefore we sought to determine whether they also occur after CCI injury in the rodent brain. At 7 days post-injury when controlling for injury severity, we found significant FA increases in the subcortical white matter compared to pre-injury that extended almost the entire rostral-caudal extent of the brain (Fig. 7A–D, $P<0.05$ FWE corrected). This included the anterior commissure, thalamus, internal capsule and cerebral peduncle. Increased AD was the clear driver of the increased anisotropy in these regions (Fig. 7E, $P<0.01$) rather than RD which remained unchanged (Fig. 7F, $P>0.05$), while MD showed highly variable, but significant increases (Fig. 7G, $P<0.05$), possibly indicating residual edema within some brains at 7 days post-injury. An investigation of the injury severity dependence for the increase in FA revealed a significant positive association within the contralateral internal capsule (Fig. 7H–J, $r^2=0.78$, $P<0.001$) which contrasts to the significant negative association between injury severity and RD and MD within the same region at 7 days (Fig. 2F, 2I).

Subcortical increases in FA persisted chronically at 4 weeks post-injury, occurring in those regions listed above for 7 days post-injury with additional involvement of the caudate putamen and posterior corpus callosum, as well as marked involvement of the cortico-spinal tract, from internal capsule to cerebral peduncle (Fig. 8A–D, $P<0.05$, FWE corrected). Unlike at 7 days, AD remained unchanged from pre-injury in these regions of FA increase, although it was highly variable compared to RD (Fig. 8E,F). MD was also unaffected, likely indicating complete resolution of edema within these regions by this post-injury time (Fig. 8G). The severity dependence of the FA increase measured at 7 days did not persist to 4 weeks post-injury (not shown).

Neither changes in the tensor mode or gliosis account for FA increases after TBI

One possibility that might explain the FA increase is a reduction in the effect that multiple crossing fibers (via axonal degeneration) has on the partial volume averaging of the signal through the image voxel, resulting in increased FA. A major limitation of the single-tensor model is that it is relatively insensitive to multiple fiber orientations within the same voxel. Modelling two fibers per voxel does show crossing points throughout the rat brain regardless of injury (Fig. 8H–M, crossing red/blues lines in the same voxel). One simple parametric that has been used to characterize this is tensor shape, quantified through the tensor mode (MO). It is a metric orthogonal to FA that extends from planar anisotropy (two large eigenvalues and one small to describe a flattened tensor shape) at a value of −1, to linear anisotropy (one large eigenvalue value, two small) at a value of +1 (Ennis and Kindlmann, 2006; Kindlmann et al., 2007). We hypothesized that if a reduction in the number of crossing fibers occurring due to deafferentation results in an increase in FA (due to reduced partial volume averaging effect), then this would be identified through a co-localized increase in MO (more linear anisotropy, reflecting a single population of fibers) when comparing pre- to post-injury values. Given the potential confounding influence of the increased MD in the

regions of increased FA at 7 days post-injury (Fig. 7G) we elected to confine our TBSS analysis of this metric to 4 weeks post-injury when MD was not different from control (Fig. 8G). The results revealed that while MO was indeed significantly increased from pre-injury levels in ipsilateral cingulum and bilateral edges of the external capsule (Fig. 8N), there was no overlap to the regions of increased FA at this time post-injury (Fig. 8A), indicating that fiber degeneration was unlikely to be a factor resulting in increased FA values. One point to support the likely validity of this metric after TBI, is the significant post-injury decrease in MO that was found in regions adjacent to the injury site, as well as bilateral in anterior regions, indicating fiber disorganization within this normally uniformly organized structure of parallel fibers (Fig. 8N).

Grey matter increases in anisotropy after experimental TBI have been shown to be associated with the coherent organization of reactive astrocytes (Budde et al., 2011). While no glial association was found for changes in corpus callosum white matter FA in that prior work, it remains possible that gliosis might underlie the FA increases we found in thalamic and internal capsule white matter regions (Fig. 8A). Immunohistochemistry for GFAP-positive reactive astrocytes surveyed in 3 rats at 4 weeks post-injury and 3 naive rats revealed persistent ipsilateral thalamic gliosis (Fig. 9A,D) typical of this CCI injury model compared to sham-injured controls (Chen et al., 2003). However, no contralateral thalamic gliosis was present, and none or very limited GFAP-positive astrocytes were noted bilaterally within the internal capsule (Fig. 9B,C,E,F). Given the prevalent, bilateral nature of the post-injury white matter FA changes found in the current work, it therefore appears unlikely that gliosis is a significant factor in these white matter changes.

Increased fiber tract density occurs in regions of FA increase after TBI

There have been some reports of increased FA clinically (Bazarian et al., 2007; Henry et al., 2011; Mayer et al., 2010; Wilde et al., 2008) and in light of work showing that increased FA is associated with increases in fiber tract density (FTD) in owl monkey brain (Choe et al., 2012), we investigated this possibility in the current data set before and at 4 weeks post-injury. In agreement with the retrograde tract-tracing work presented earlier (Fig. 6), FTD maps created by whole brain deterministic tractography of FA data (Fig. 10A–C) revealed a significant decrease in fiber density within bilateral corpus callosum and fornix at 28 days post-injury when compared to pre-injury (Fig. 10B–D, $P<0.05$, corrected). More interestingly however, significant increases in FTD were also evident in bilateral regions of the caudate putamen, thalamus and internal capsule and extending to the ipsilateral cerebral peduncle (Fig. 10E, $P<0.05$, FWE corrected). These same regions were spatially consistent with areas of FA increase on the corresponding FA contrast maps (Fig. 8A), suggesting an association between FA and FTD after TBI. Interrogating the FTD data for a dependence on injury severity revealed a significant negative association within the genu of the corpus callosum and extending posteriorly to the ipsilateral external capsule under the primary injury site (Fig. 10F, $P<0.05$, corrected; Fig. 10G, $r^2=0.80$, $P<0.001$).

Fiber tract length is greater in regions of increased FA

Given the *ex vivo* reported finding in the rodent epilepsy models that increased FA is associated with sprouting fibers (Laitinen et al., 2010), we sought to uncover whether

average fiber length was increased in regions of higher FA, possibly as a reflection of earlier cortical axonal sprouting that occurs in the TBI model used here (Harris et al., 2010b). We found that the average length of fibers seeded from all white matter regions with significantly increased FA within each brain at 4 weeks post-injury was 7.07mm ±0.20, significantly greater than 5.47 ±0.22mm that was obtained in the same brain regions seeded prior to injury ($P<0.001$, 2-tailed t test). This occurred independent of injury severity ($P>0.05$) in agreement with the absence of any association between subcortical white matter FTD and injury severity (Fig. 10F). Finally, the consistent finding of injury-related altered diffusivity within the internal capsule/peduncle found in the earlier data (Fig. 7A, 8A, 10E) that appeared to be particularly associated with injury severity within the contralateral tracts (Fig. 2D, 2G, 7H, 10E) prompted us to determine fiber length measurements in this region. We warped the internal capsule regions from a parcellated rat atlas to the native space of each rat and determined mean fiber length from these seed regions. We found that the mean length of fibers seeded from the ipsilateral internal capsule at 4 weeks post-injury was significantly lower than pre-injury (3.58 ±0.13 versus 5.07 ±0.22mm, respectively, $P<0.001$, 2-tailed t test; supp. Fig. S1) while the contralateral internal capsule-seeded mean fiber length was significantly greater than pre-injury (6.24 ±0.24 versus 5.21 ±0.18mm, respectively, $P<0.01$, 2-tailed t test; supp. Fig. S1). Neither dataset was associated with injury severity ($P>0.05$).

Discussion

FA Reduction- Fiber Tract Disorganization

The major novel findings in the current work are bi-directional changes in FA after injury as well as severity dependent changes in the DTI indices and they add to our knowledge on imaging biomarkers after TBI. We found persistent reductions in FA within corpus callosum regions after CCI injury similar to prior findings in both the mouse and rat version of this TBI model at 24hrs and 2 months post-injury respectively (Budde et al., 2011; MacDonald et al., 2007). We also found that FA reductions are driven by an increase in RD acutely, but by increased RD and MD chronically. Early increases in RD are likely to occur due to the reduced impedance to diffusion resulting from demyelination that we showed is already well-established by 3 days post-injury, similar to RD changes after optic nerve damage (Song et al., 2002). The persistent reduction in FA to 4 weeks post-injury that is driven by changes in all DTI scalars measured reflects a loss of axon fibers within the corpus callosum, as supported by the reduction in neurofilaments, reduced tract-traced-labelled cells, and the reduction in FTD obtained through *in vivo* tractography.

Novel to the understanding of this model was the consideration of injury severity in the statistical analyses of the data. We found that greater FA decreases in ipsilateral corpus callosum occurred in more severely injured rats regardless of post-injury time-point, and increases in AD, RD and MD chronically were associated with more severe injury, similar to observations after clinical TBI (Håberg et al., 2014; Rutgers et al., 2008). Furthermore, we found that additional contralateral regions of corpus callosum exhibited this severity dependence relationship for FA at 4 weeks post-injury but not at 1 week, suggesting that ongoing degeneration from the ipsi- to the contra-lateral hemisphere that occurs in more

severely injured rats underlies this result. This conclusion is supported by the measured increased diffusivity along the axon tracts (AD), loss of neurofilaments shown by immunohistochemistry, loss of fiber tracts shown by *in vivo* tractography within this region. These are important changes that might well have been missed by a region-of-interest (ROI) based approach that has been used in the majority of prior experimental TBI studies. These results are all somewhat expected and agree well with the interhemispheric functional disconnection that occurs from both 7 and 28 days in these same animals (Harris et al, 2016,) and in good agreement with the loss of callosal function predicted by lower FA after pediatric TBI in humans (Dennis et al., 2015). It will be useful in future work to use planned variations in injury severity to determine the degree to which DTI measures are sensitive to axonal disturbances compared to histology readouts.

Whole brain white matter analysis unconstrained by FA changes revealed increases in AD, RD and MD at 4 weeks that were widespread bilaterally with corpus callosum and subcortical structures. Importantly, many of these areas were non-overlapping with regions of reduced FA, and suggest that consideration of the principal eigenvalues alone is warranted in analysis of white matter pathology post-TBI, rather than limiting their use to explaining the likely pathology underlying changes in FA. However, given that variable increases in all three indices underpinned the observed reductions in ipsilateral FA, it is possible that the absence of a more widespread change in FA within regions that show alteration in its component eigenvalues, occurs due to a commensurate change in all three parameters resulting in no net change in FA. This would suggest that in some circumstances FA may underestimate the degree of white matter damage. Regardless, this tract-based analysis has shown that the degree and extent of white matter injury after CCI injury is far more widespread than is often appreciated by ROI-based analysis of DTI or by immunohistochemistry. The extent of change demonstrated in this DTI study is in fact closer to the axon degeneration studies conducted with silver staining techniques after CCI injury (Hall et al., 2008, 2005; Matthews et al., 1998). The extent of the delineated reduction in white matter connectivity that extends to the contralataral hemisphere does in fact coincide temporally and regionally with functional disconnection in these same rats (Harris et al, 2016), and would suggest that a structural-functional relationship remains despite injury. However, a structural-fucntional relationship is complex in this model (Harris et al, 2016), and a thorough voxel-based approach between these data would be required to more fully explore whether this occurs on both a regional, as well as a global level.

FA Increases

Especially novel to this study is the observed injury-related increase in FA within regions spatially distinct from those with FA reductions, and at both acute and chronic post-injury time–points. TBI-induced FA increases in white matter tracts have been reported clinically (Cubon et al., 2011; Ling et al., 2012; Lipton et al., 2012; Mayer et al., 2015; Messé et al., 2010; Sidaros et al., 2008). FA increases after experimental TBI are reported after experimental blast or fluid percussion injury (Johnstone et al., 2015; Rubovitch et al., 2011), in the thalamus acutely after CCI injury (Xu et al., 2011) and in ipsilateral cortical grey matter chronically after CCI injury (Budde et al., 2011). These prior experimental TBI studies report grey matter changes in FA, and as such these measurements are likely to be

confounded by the contribution of gliosis to anisotropy, as occurs within perilesional grey matter tissue after injury (Budde et al., 2011). Although the morphological change in axonal structure or extracellular space that may underlie increases in white matter FA is not understood, functionally it has been associated with training-induced effects in normal volunteers (Schlegel et al., 2012; Scholz et al., 2009) and possibly with activity dependence in mice trained on a rotarod (Scholz et al., 2015). We observed widespread subcortical increases bilaterally at 1 week post-injury that persisted at 4 weeks, and similar changes have been shown subcortically after mild clinical TBI (Lipton et al., 2012). However, there are many potential contributions to the magnetic resonance signal that may confound the interpretation of DTI, for example partial volume effects (Vos et al., 2011), iron/hemosiderin-related products (Rulseh et al., 2013), gliosis (Budde et al., 2011), fiber degeneration (Douaud et al., 2009), among other factors. Clearly all of these will potentially affect the interpretation of the current data in the CCI model since iron accumulation (Onyszchuk et al., 2009) gliosis (Chen et al., 2003) and degeneration (Hall et al., 2008, 2005; Matthews et al., 1998) have all been shown to be present. However, the widespread bilateral and antero-posterior nature of the FA increases that we found do not easily fit the interpretation that increases in FA are artifacts of a confounded signal. Such an explanation here would be at odds with the discordant spatial patterns of increased FA and observed gliosis. Gliosis, though widespread, is very heavy unilaterally within the thalamus at 4 weeks post-CCI, Fig. 9. (Chen et al., 2003) and not different in the internal capsule (Fig. 9). Similar findings have been shown for iron accumulation 2 months following CCI in aged mice (Onyszchuk et al., 2009).

Structural Reorganization?

In light of our findings, it is tempting to consider an alternative theory of post-TBI pathogenesis, namely that increased FA indicates a degree of structural remodeling. Significant spontaneous axon sprouting occurs within the ipsilesional cortical grey and white matter after rodent CCI injury (Harris et al., 2010b). Although sprouting at the level of the thalamus or corticospinal tract (CST) has not been investigated in this model, a sustained regenerative attempt was shown in the long pyramidal tracts in the medulla and pons after feline fluid percussion injury (Christman et al., 1997), suggesting that lower brain structures may well attempt to regenerate after injury. Structural remodeling is an attractive hypothesis to explain the spontaneous behavioral recovery that occurs in this model (Harris et al., 2010a). Even small alterations in major fiber projection pathways will likely have a significant effect on higher brain function. This hypothesis is compatible with the recent finding of a large degree of functional hyper-connectivity within bilateral cortical and subcortical regions at 7–14 days after CCI injury when compared to pre-injury (Harris et al, 2016). In that study from the same rats used in the current study and with overlapping time-points, the data showed that early after injury the brain is likely to be connectively promiscuous, with decreases in the shortest path between brain regions and increased reliance on local connectivity, as indicated by increased nodal clustering coefficient at more chronic post-injury times, Given that the data from the present study were acquired in the same animals and at the same time points as the prior resting state functional MRI study, the time-course of the DTI results do suggest that a structural-functional association may persist in the period of post-injury reorganization. However, a postulated relationship between

structural reorganization in subcortical structures suggested herein and functional hyperconnectivity in the same model (Harris et al, 2016) would require further investigation in order to demonstrate a causal association.

The present results show that in addition to subcortical increases in FA, higher FA values in the contralateral CST were associated with more severe injury at 7 days. This was also commensurate with lower RD and MD values in this region in more severely injured rats at 7 days. Greater FA values persisted in the contralateral CST to 4 weeks, and we showed that this was associated with increased fiber tract density in both CST's as well as caudate and thalamic white matter regions. The functional significance of these changes remain unclear, but similar FA findings have been reported clinically; increased FA occurred in internal capsule when assessed 1–2 years after mild (Lo et al., 2009) and severe TBI (Sidaros et al., 2008), and larger FA values in the cerebral peduncle were associated with better outcome after TBI (Sidaros et al., 2008). Whether or not reduced RD and MD at 7 days are also potential correlates of white matter reorganization, or simply a reflection of improved fiber integrity (higher membrane resistance to radial diffusion) and/or increased fiber number, remains to be investigated.

Data on the functional significance of increased FA is scarce, but better performance on a postural control task was associated with higher FA in specific sensorimotor pathways, including the internal capsule, in young TBI patients (Caeyenberghs et al., 2009). Similarly, transcranial direct current stimulation in stroke victims increased FA in alternative motor pathways associated with the internal capsule and correlated with improved functional scores (Zheng and Schlaug, 2015). Clearly, structural reorganization within the CST and after TBI would have a large impact on brain function. In the current study, the post-injury bilateral increases in fiber density in the internal capsule might be tentatively considered as one morphologic correlate of such a reorganization. The same might be said of the increased length of fibers arising from the contralateral internal capsule. The lower post-injury fiber length in the ipsilateral capsule would suggest a continued ipsilateral disconnection among some projection tracts, and that there is possibly some compensation for this by the contralateral circuitry. Indeed, functional connectivity analysis of these rats showed that the contralateral cortex does play a central role in the post-injury period of hyperconnectivity (Harris et al. 2016). It will be of interest in future work to determine if contralaterally raised FA values are causally involved in ipsi-to-contralateral reorganization of the cortical forelimb map that occurs early after injury in this TBI model (Harris et al., 2013). Finally, considering the disorganization/reorganization hypothesis of decreased/increased FA, the finding of an association between injury severity and increased FA at 7 days, and to decreased FA at all times post-injury would suggest that despite greater disorganization after more severe injury, greater reorganization occurs at 7 days possibly to offset the greater damage in order to improve function. Functional evidence from these same rats show greater local connectedness (lower characteristic shortest path and greater mean clustering coefficient) after moderate/severe injury when compared to milder injury (Harris et al, 2016) further supporting the idea that a structural-functional relationship is maintained in the post-injury period following experiment TBI.

In conclusion, we have shown that a tract-based analysis of DTI data after CCI injury provides a more complete picture of the widespread and progressive axonal pathology that occurs in this model. We found both decreases and increases in FA within spatially distinct regions that correlated to injury severity, and that FTD and fiber tract length was associated with these findings. Considering published functional data from the same rats showing disconnection and significant hyperconnectivity (Harris et al, 2016), a structural-functional relationship appears to be maintained in the post-injury period of reorganization. The widespread nature of these structural data and the prior published functional data in this model of experimental TBI refute the dogma that the model is entirely focal in nature, and further validate its use as a clinically-relevant model of TBI.

Supplementary Material

Refer to Web version on PubMed Central for supplementary material.

Acknowledgments

We thank Josh Newman for performing the neurofilament and myelin basic protein immunohistochemistry and the UCLA *in vivo* Imaging Centre.

Funding Source: UCLA Brain Injury Research Center; NIH NINDS NS091222 & NS27544. The project described was also supported in part by the MRI Core of the Semel Institute of Neuroscience at UCLA which is supported by Intellectual Development and Disabilities Research Center grant number U54HD087101-01 from the Eunice Kennedy Shriver National Institute of Child Health and Human Development. The content is solely the responsibility of the authors and does not necessarily represent the official views of the Eunice Kennedy Shriver National Institute of Child Health and Human Development or the National Institutes of Health. NGH is a fellow of The Center for Neuroskills, Bakersfield, California

Bibliography

Bazarian JJ, Zhong J, Blyth B, Zhu T, Kavcic V, Peterson D. Diffusion tensor imaging detects clinically important axonal damage after mild traumatic brain injury: a pilot study. J Neurotrauma. 2007; 24:1447–1459. DOI: 10.1089/neu.2007.0241 [PubMed: 17892407]

Behrens TEJ, Berg HJ, Jbabdi S, Rushworth MFS, Woolrich MW. Probabilistic diffusion tractography with multiple fibre orientations: What can we gain? Neuroimage. 2007; 34:144–55. DOI: 10.1016/j.neuroimage.2006.09.018 [PubMed: 17070705]

Behrens TEJ, Woolrich MW, Jenkinson M, Johansen-Berg H, Nunes RG, Clare S, Matthews PM, Brady JM, Smith SM. Characterization and propagation of uncertainty in diffusion-weighted MR imaging. Magn Reson Med. 2003; 50:1077–88. DOI: 10.1002/mrm.10609 [PubMed: 14587019]

Budde MD, Janes L, Gold E, Turtzo LC, Frank JA. The contribution of gliosis to diffusion tensor anisotropy and tractography following traumatic brain injury: validation in the rat using Fourier analysis of stained tissue sections. Brain. 2011; doi: 10.1093/brain/awr161

Budde MD, Xie M, Cross AH, Song SK. Axial diffusivity is the primary correlate of axonal injury in the experimental autoimmune encephalomyelitis spinal cord: a quantitative pixelwise analysis. J Neurosci. 2009; 29:2805–13. DOI: 10.1523/JNEUROSCI.4605-08.2009 [PubMed: 19261876]

Caeyenberghs K, Leemans A, Geurts M, Taymans T, Linden C Vander, Smits-Engelsman BCM, Sunaert S, Swinnen SP. Brain-behavior relationships in young traumatic brain injury patients: DTI metrics are highly correlated with postural control. Hum Brain Mapp. 2009; 31:992–1002. DOI: 10.1002/hbm.20911 [PubMed: 19998364]

Chen S, Pickard JD, Harris NG. Time course of cellular pathology after controlled cortical impact injury. Exp Neurol. 2003; 182:87–102. [PubMed: 12821379]

Chen S, Richards HK, Smielewski P, Pickard JD, Harris NG. Preventing flow-Metabolism uncoupling acutely reduces evolving axonal injury after traumatic brain injury. J Neurotrauma. 2002; 19:1300.

Chen SF, Richards HK, Smielewski P, Johnstrom P, Salvador R, Pickard JD, Harris NG. Relationship between flow-metabolism uncoupling and evolving axonal injury after experimental traumatic brain injury. J Cereb Blood Flow Metab. 2004; 24:1025–1036. [PubMed: 15356423]

Chiang CW, Wang Y, Sun P, Lin TH, Trinkaus K, Cross AH, Song SK. Quantifying white matter tract diffusion parameters in the presence of increased extra-fiber cellularity and vasogenic edema. Neuroimage. 2014; 101:310–9. DOI: 10.1016/j.neuroimage.2014.06.064 [PubMed: 25017446]

Choe AS, Stepniewska I, Colvin DC, Ding Z, Anderson AW. Validation of diffusion tensor MRI in the central nervous system using light microscopy: Quantitative comparison of fiber properties. NMR Biomed. 2012; 25:900–908. DOI: 10.1002/nbm.1810 [PubMed: 22246940]

Christman CWW, Salvant JBB, Walker SAa, Povlishock JTT. Characterization of a prolonged regenerative attempt by diffusely injured axons following traumatic brain injury in adult cat: a light and electron microscopic immunocytochemical study. Acta Neuropathol(Berl). 1997; 94:329–337. DOI: 10.1007/s004010050715 [PubMed: 9341933]

Crum WR, Giampietro VP, Smith EJ, Gorenkova N, Stroemer RP, Modo M. A comparison of automated anatomical-behavioural mapping methods in a rodent model of stroke. J Neurosci Methods. 2013; 218:170–183. DOI: 10.1016/j.jneumeth.2013.05.009 [PubMed: 23727124]

Cubon VA, Putukian M, Boyer C, Dettwiler A. A Diffusion Tensor Imaging Study on the White Matter Skeleton in Individuals with Sports-Related Concussion. J Neurotrauma. 2011; 28:189–201. DOI: 10.1089/neu.2010.1430 [PubMed: 21083414]

Dennis EL, Ellis MU, Marion SD, Jin Y, Moran L, Olsen A, Kernan C, Babikian T, Mink R, Babbitt C, Johnson J, Giza CC, Thompson PM, Asarnow RF. Callosal Function in Pediatric Traumatic Brain Injury Linked to Disrupted White Matter Integrity. J Neurosci. 2015; 35:10202–10211. DOI: 10.1523/JNEUROSCI.1595-15.2015 [PubMed: 26180196]

Douaud G, Behrens TE, Poupon C, Cointepas Y, Jbabdi S, Gaura V, Golestani N, Krystkowiak P, Verny C, Damier P, Bachoud-Lévi AC, Hantraye P, Remy P. In vivo evidence for the selective subcortical degeneration in Huntington's disease. Neuroimage. 2009; 46:958–966. DOI: 10.1016/j.neuroimage.2009.03.044 [PubMed: 19332141]

Ennis DB, Kindlmann G. Orthogonal tensor invariants and the analysis of diffusion tensor magnetic resonance images. Magn Reson Med. 2006; 55:136–146. DOI: 10.1002/mrm.20741 [PubMed: 16342267]

Håberg AK, Olsen A, Moen KG, Schirmer-Mikalsen K, Visser E, Finnanger TG, Evensen KAI, Skandsen T, Vik A, Eikenes L. White matter microstructure in chronic moderate-to-severe traumatic brain injury: Impact of acute-phase injury-related variables and associations with outcome measures. J Neurosci Res. 2014; n/a–n/a. doi: 10.1002/jnr.23534

Hall ED, Bryant YD, Cho W, Sullivan PG. Evolution of post-traumatic neurodegeneration after controlled cortical impact traumatic brain injury in mice and rats as assessed by the de Olmos silver and fluorojade staining methods. J Neurotrauma. 2008; 25:235–47. DOI: 10.1089/neu.2007.0383 [PubMed: 18352837]

Hall ED, Sullivan PG, Gibson TR, Pavel KM, Thompson BM, Scheff SW. Spatial and temporal characteristics of neurodegeneration after controlled cortical impact in mice: more than a focal brain injury. J Neurotrauma. 2005; 22:252–65. DOI: 10.1089/neu.2005.22.252 [PubMed: 15716631]

Harris NG, Chen S-F, Pickard J. Cortical Reorganisation after Experimental Traumatic Brain Injury: A Functional Autoradiography Study. J Neurotrauma. 2013; doi: 10.1089/neu.2012.2785

Harris NG, Hovda DA, Sutton RL. Acute deficits in transcallosal connectivity endure chronically after experimental brain injury in the rat: a dti tractography study. J Neurotrauma. 2009; 26:A37.

Harris NG, Mironova YA, Chen SF, Richards HK, Pickard JD. Preventing flow-metabolism uncoupling acutely reduces axonal injury after traumatic brain injury. J Neurotrauma. 2012; 29:1469–82. DOI: 10.1089/neu.2011.2161 [PubMed: 22321027]

Harris NG, Mironova YA, Hovda DA, Sutton RL. Chondroitinase ABC enhances pericontusion axonal sprouting but does not confer robust improvements in behavioral recovery. J Neurotrauma. 2010a; 27:1–12. DOI: 10.1089/neu.2010.1470 [PubMed: 19698073]

Harris NG, Mironova YA, Hovda DA, Sutton RL. Pericontusion axon sprouting is spatially and temporally consistent with a growth-permissive environment after traumatic brain injury. J

Neuropathol Exp Neurol. 2010b; 69:139–154. DOI: 10.1097/NEN.0b013e3181cb5bee [PubMed: 20084019]

Harris NG, Verley DR, Gutman BA, Thompson PM, Yeh HJ, Browne J. Disconnection and hyper-connectivity underlie reorganization after experiment TBI: a rodent functional connectomic analysis. Exp Neurol. 2016; 277:124–138. DOI: 10.1016/j.expneurol.2015.12.020 [PubMed: 26730520]

Henry LC, Tremblay J, Tremblay S, Lee A, Brun C, Lepore N, Theoret H, Ellemberg D, Lassonde M. Acute and Chronic Changes in Diffusivity Measures after Sports Concussion. J Neurotrauma. 2011; 28:2049–2059. DOI: 10.1089/neu.2011.1836 [PubMed: 21864134]

Jenkinson M, Bannister P, Brady M, Smith S. Improved optimization for the robust and accurate linear registration and motion correction of brain images. Neuroimage. 2002; 17:825–41. [PubMed: 12377157]

Jenkinson M, Smith S. A global optimisation method for robust affine registration of brain images. Med Image Anal. 2001; 5:143–56. [PubMed: 11516708]

Johnstone V, Wright DK, Wong KK, O'Brien TJ, Rajan R, Shultz SR. Experimental traumatic brain injury results in long-term recovery of functional responsiveness in sensory cortex but persisting structural changes and sensorimotor, cognitive, and emotional deficits. J Neurotrauma. 2015; 1346:1–38. DOI: 10.1089/neu.2014.3785

Kindlmann G, Ennis DB, Whitaker RT, Westin C. Diffusion Tensor Analysis With Invariant Gradients and Rotation Tangents. IEEE Trans Med Imaging. 2007; 26:1483–1499. [PubMed: 18041264]

Laitinen T, Sierra A, Bolkvadze T, Pitkänen A, Gröhn O. Diffusion tensor imaging detects chronic microstructural changes in white and gray matter after traumatic brain injury in rat. Front Neurosci. 2015; 9:1–12. DOI: 10.3389/fnins.2015.00128 [PubMed: 25653585]

Laitinen T, Sierra A, Pitkänen A, Gröhn O. Diffusion Tensor MRI of Axonal Plasticity in the Rat Hippocampus. Neuroimage. 2010; 51:521–30. DOI: 10.1016/j.neuroimage.2010.02.077 [PubMed: 20211740]

Ling JM, Peña A, Yeo Ra, Merideth FL, Klimaj S, Gasparovic C, Mayer AR. Biomarkers of increased diffusion anisotropy in semi-acute mild traumatic brain injury: A longitudinal perspective. Brain. 2012; 135:1281–1292. DOI: 10.1093/brain/aws073 [PubMed: 22505633]

Lipton ML, Kim N, Park YK, Hulkower MB, Gardin TM, Shifteh K, Kim M, Zimmerman ME, Lipton RB, Branch CA. Robust detection of traumatic axonal injury in individual mild traumatic brain injury patients: Intersubject variation, change over time and bidirectional changes in anisotropy. Brain Imaging Behav. 2012; 6:329–342. DOI: 10.1007/s11682-012-9175-2 [PubMed: 22684769]

Lo C, Shifteh K, Gold T, Bello Ja, Lipton ML. Diffusion tensor imaging abnormalities in patients with mild traumatic brain injury and neurocognitive impairment. J Comput Assist Tomogr. 2009; 33:293–297. DOI: 10.1097/RCT.0b013e31817579d1 [PubMed: 19346863]

Long JA, Watts LT, Chemello J, Huang S, Shen Q, Duong TQ. Multiparametric and longitudinal MRI characterization of mild traumatic brain injury in rats. J Neurotrauma. 2015; 32:598–607. DOI: 10.1089/neu.2014.3563 [PubMed: 25203249]

Mac Donald CL, Johnson AM, Cooper D, Nelson EC, Werner NJ, Shimony JS, Snyder AZ, Raichle ME, Witherow JR, Fang R, Flaherty SF, Brody DL. Detection of blast-related traumatic brain injury in U.S. military personnel. N Engl J Med. 2011; 364:2091–100. DOI: 10.1056/NEJMoa1008069 [PubMed: 21631321]

Mac MacDonald CL, Dikranian K, Song SK, Bayly PV, Holtzman DM, Brody DL, Brody DL. Detection of traumatic axonal injury with diffusion tensor imaging in a mouse model of traumatic brain injury. Exp Neurol. 2007; 205:116–31. DOI: 10.1016/j.expneurol.2007.01.035 [PubMed: 17368446]

Matthews MA, Carey ME, Soblosky JS, Davidson JF, Tabor SL. Focal brain injury and its effects on cerebral mantle, neurons, and fiber tracks. Brain Res. 1998; 794:1–18. [PubMed: 9630470]

Mayer AR, Hanlon FM, Ling JM. Gray matter abnormalities in pediatric mild traumatic brain injury. J Neurotrauma. 2015; 32:723–30. DOI: 10.1089/neu.2014.3534 [PubMed: 25313896]

Mayer AR, Ling J, Mannell MV, Gasparovic C, Phillips JP, Doezema D, Reichard R, Yeo RA. A prospective diffusion tensor imaging study in mild traumatic brain injury. Neurology. 2010; doi: 10.1212/WNL.0b013e3181d0ccdd

Messé A, Caplain S, Paradot G, Garrigue D, Mineo J-F, Soto Ares G, Ducreux D, Vignaud F, Rozec G, Desal H, Pélégrini-Issac M, Montreuil M, Benali H, Lehéricy S. Diffusion tensor imaging and white matter lesions at the subacute stage in mild traumatic brain injury with persistent neurobehavioral impairment. Hum Brain Mapp. 2010; doi: 10.1002/hbm.21092

Mori S, Crain BJ, Chacko VP, van Zijl PC. Three-dimensional tracking of axonal projections in the brain by magnetic resonance imaging. Ann Neurol. 1999; 45:265–9. [PubMed: 9989633]

Onyszchuk G, LeVine SM, Brooks WM, Berman NEJ. Post-acute pathological changes in the thalamus and internal capsule in aged mice following controlled cortical impact injury: A magnetic resonance imaging, iron histochemical, and glial immunohistochemical study. Neurosci Lett. 2009; 452:204–208. DOI: 10.1016/j.neulet.2009.01.049 [PubMed: 19383440]

Paxinos, G.; Watson, C. The rat brain in stereotaxic coordinates. Academic Press; New York: 1997.

Rubovitch V, Ten-Bosch M, Zohar O, Harrison CR, Tempel-Brami C, Stein E, Hoffer BJ, Balaban CD, Schreiber S, Chiu WT, Pick CG. A mouse model of blast-induced mild traumatic brain injury. Exp Neurol. 2011; 232:280–289. DOI: 10.1016/j.expneurol.2011.09.018 [PubMed: 21946269]

Rulseh AM, Keller J, Tintěra J, Kožíšek M, Vymazal J. Chasing shadows: what determines DTI metrics in gray matter regions? An in vitro and in vivo study. J Magn Reson Imaging. 2013; 38:1103–10. DOI: 10.1002/jmri.24065 [PubMed: 23440865]

Rutgers DR, Fillard P, Paradot G, Tadié M, Lasjaunias P, Ducreux D. Diffusion tensor imaging characteristics of the corpus callosum in mild, moderate, and severe traumatic brain injury. AJNR Am J Neuroradiol. 2008; 29:1730–5. DOI: 10.3174/ajnr.A1213 [PubMed: 18617586]

Schlegel, Aa; Rudelson, JJ.; Tse, PU. White Matter Structure Changes as Adults Learn a Second Language. J Cogn Neurosci. 2012; 24:1664–1670. DOI: 10.1162/jocn_a_00240 [PubMed: 22571459]

Scholz J, Klein MC, Behrens TEJ, Johansen-Berg H. Training induces changes in white-matter architecture. Nat Neurosci. 2009; 12:1370–1371. DOI: 10.1038/nn.2412 [PubMed: 19820707]

Scholz J, Niibori Y, Frankland WP, Lerch PJ. Rotarod training in mice is associated with changes in brain structure observable with multimodal MRI. Neuroimage. 2015; 107:182–189. DOI: 10.1016/j.neuroimage.2014.12.003 [PubMed: 25497397]

Sidaros A, Engberg AW, Sidaros K, Liptrot MG, Herning M, Petersen P, Paulson OB, Jernigan TL, Rostrup E. Diffusion tensor imaging during recovery from severe traumatic brain injury and relation to clinical outcome: a longitudinal study. Brain. 2008; 131:559–572. DOI: 10.1093/brain/awm294 [PubMed: 18083753]

Sierra A, Laitinen T, Lehtimäki K, Rieppo L, Pitkänen A, Gröhn O. Diffusion tensor MRI with tract-based spatial statistics and histology reveals undiscovered lesioned areas in kainate model of epilepsy in rat. Brain Struct Funct. 2011; doi: 10.1007/s00429-010-0299-0

Smith SM. Fast robust automated brain extraction. Hum Brain Mapp. 2002; 17:143–55. DOI: 10.1002/hbm.10062 [PubMed: 12391568]

Smith SM, Jenkinson M, Johansen-Berg H, Rueckert D, Nichols TE, Mackay CE, Watkins KE, Ciccarelli O, Cader MZ, Matthews PM, Behrens TEJ. Tract-based spatial statistics: voxelwise analysis of multi-subject diffusion data. Neuroimage. 2006; 31:1487–505. DOI: 10.1016/j.neuroimage.2006.02.024 [PubMed: 16624579]

Song SK, Sun SW, Ramsbottom MJ, Chang C, Russell J, Cross AH. Dysmyelination revealed through MRI as increased radial (but unchanged axial) diffusion of water. Neuroimage. 2002; 17:1429–36. [PubMed: 12414282]

Valdés-Hernández PA, Sumiyoshi A, Nonaka H, Haga R, Aubert-Vásquez E, Ogawa T, Iturria-Medina Y, Riera JJ, Kawashima R. An in vivo MRI Template Set for Morphometry, Tissue Segmentation, and fMRI Localization in Rats. Front Neuroinform. 2011; 5:26.doi: 10.3389/fninf.2011.00026 [PubMed: 22275894]

Vos SB, Jones DK, Viergever Ma, Leemans A. Partial volume effect as a hidden covariate in DTI analyses. Neuroimage. 2011; 55:1566–1576. DOI: 10.1016/j.neuroimage.2011.01.048 [PubMed: 21262366]

Wilde EA, McCauley SR, Hunter JV, Bigler ED, Chu Z, Wang ZJ, Hanten GR, Troyanskaya M, Yallampalli R, Li X, Chia J, Levin HS. Diffusion tensor imaging of acute mild traumatic brain

injury in adolescents. Neurology. 2008; 70:948–55. DOI: 10.1212/01.wnl.0000305961.68029.54 [PubMed: 18347317]

Winkler AM, Ridgway GR, Webster MA, Smith SM, Nichols TE. Permutation inference for the general linear model. Neuroimage. 2014; 92:381–97. DOI: 10.1016/j.neuroimage.2014.01.060 [PubMed: 24530839]

Xu S, Zhuo J, Racz J, Shi D, Roys S, Fiskum G, Gullapalli R. Early microstructural and metabolic changes following controlled cortical impact injury in rat: a magnetic resonance imaging and spectroscopy study. J Neurotrauma. 2011; 28:2091–102. DOI: 10.1089/neu.2010.1739 [PubMed: 21761962]

Yushkevich PA, Piven J, Hazlett HC, Smith RG, Ho S, Gee JC, Gerig G. User-guided 3D active contour segmentation of anatomical structures: significantly improved efficiency and reliability. Neuroimage. 2006; 31:1116–28. DOI: 10.1016/j.neuroimage.2006.01.015 [PubMed: 16545965]

Zheng X, Schlaug G. Structural white matter changes in descending motor tracts correlate with improvements in motor impairment after undergoing a treatment course of tDCS and physical therapy. Front Hum Neurosci. 2015; 9:229.doi: 10.3389/fnhum.2015.00229 [PubMed: 25983684]

Zhuo J, Xu S, Proctor JL, Mullins RJ, Simon JZ, Fiskum G, Gullapalli RP. Diffusion kurtosis as an in vivo imaging marker for reactive astrogliosis in traumatic brain injury. Neuroimage. 2012; 59:467–77. DOI: 10.1016/j.neuroimage.2011.07.050 [PubMed: 21835250]

Highlights

- TBSS analysis of FA, AD, RD, MO, FTD and covariate of injury severity at 1 and 4 wks
- FA decreases driven by RD acutely, but AD and RD chronically
- Region of AD and RD change greater than FA acutely, less than FA chronically
- FA increases subcortical – associated with increased fiber-tract density and length
- Data refute the dogma that CCI model of TBI is focal with limited axonal pathology

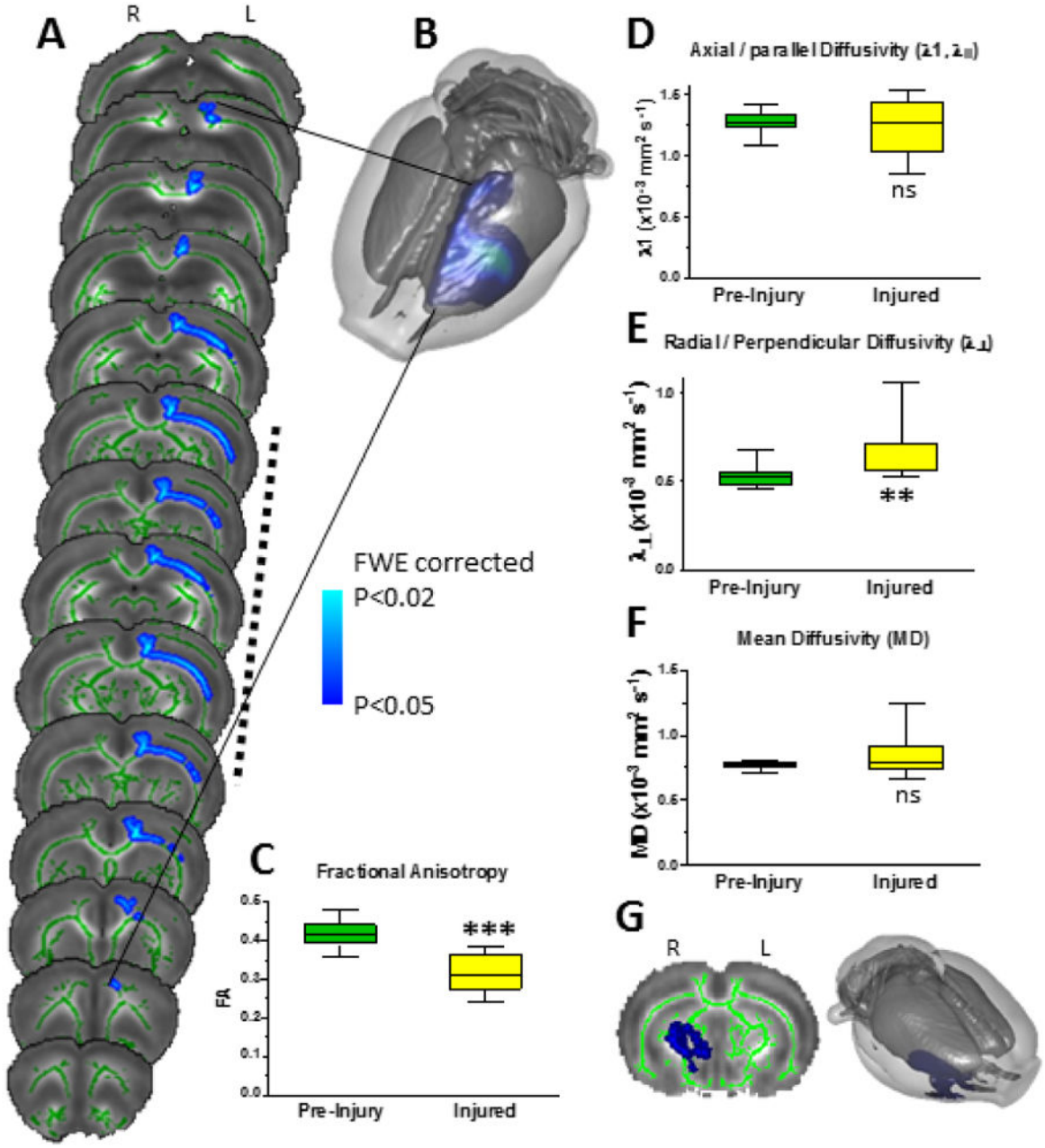

Fig. 1. CCI injury results in a unilateral reduction in corpus callosum fractional anisotropy (FA) driven by increased radial diffusivity (RD) at 7 days post-injury

TBSS analysis was used to investigate group-wise changes in DTI parameters at 7 days post-injury compared to pre-injury using voxel-wise, cluster-size-based statistical analysis (z=1.7, P<0.05, family-wise error (FWE) corrected, unpaired t test) and controlling for injury severity (contusion size). [**A**] Coronal mean pre-injury FA images overlaid with mean axonal skeleton computed from all data (green) and the post-injury region of significantly reduced FA (blue) compared to pre-injury that occurs within the primary contused region (dotted line) and in regions remote from this. [**B**] The same significant FA data projected on to the white matter surface (dark grey) of a 3D template brain (transparent/light grey). [**C**] Average

region-of-interest (ROI) FA data obtained from the significant region in [**A**] back-projected onto each rat, confirmed the group reduction in FA. [**D**] Axial diffusivity (AD), [**E**] radial diffusivity (RD), and [**F**] mean diffusivity (MD) data computed from the same regions of reduced FA in [**A**] shows that increased RD is driving the reduction in corpus callosum FA while MD remained unchanged, indicating that swelling or cell death was not a major factor. [**G**] White matter analysis of AD, RD and MD unconstrained by reductions in FA but controlling for injury severity revealed no significant changes apart from RD, which was reduced in contralateral (right) subcortical regions (blue region), although reductions in AD were just outside significance in ipsilateral corpus callosum regions (P=0.06, data not shown). Key: L- left, R- right; *** = P<0.001, ** = P<0.01, *=P<0.05, ns- not significant. Dotted line- primary region of contusion cavity.

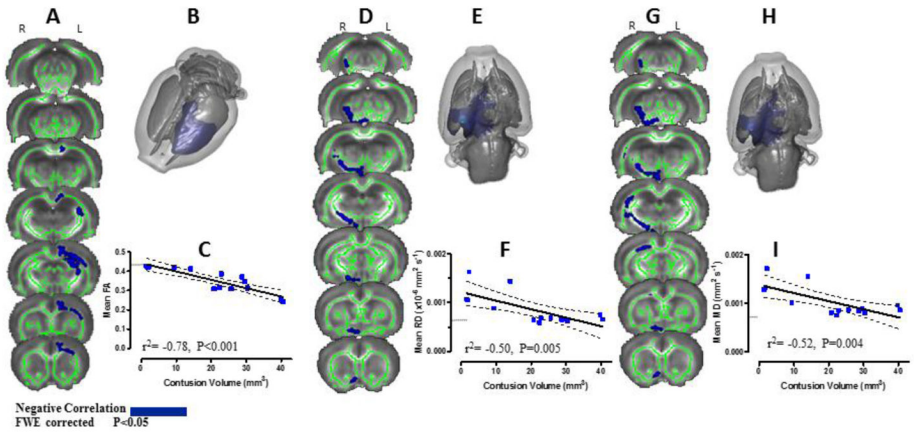

Fig. 2. Ipsilateral corpus callosum FA and contralateral internal capsule RD and MD are negatively correlated with injury severity at 7 days after injury

Regions of white matter where [**A–C**] FA, [**D–F**] RD, and [**G–I**] MD were negatively correlated (blue regions) to injury severity (contusion size) at 7 days post-injury (P<0.05). [**A**] Coronal mean pre-injury FA images overlaid with the mean axon skeleton and regions that negatively correlated (blue) to injury severity. [**B**] 3D volume projection image showing that the ipsilateral corpus callosum was negatively correlated to injury severity as confirmed in [**C**] a plot of individual brain ROI values from this region in [**A,B**] that were back-projected onto each brain. Similar negative correlations were found in contralateral internal capsule on coronal images for [**D**] RD and [**G**] MD and the associated 3D projection images of [**E**] RD and [**H**] MD and individual brain ROI data at 7 days for [**F**] RD and [**I**] MD. AD was also assessed but did not reach significance. Key: Grey horizontal line in each graph is the mean pre-injury control value for the injury-significant region.

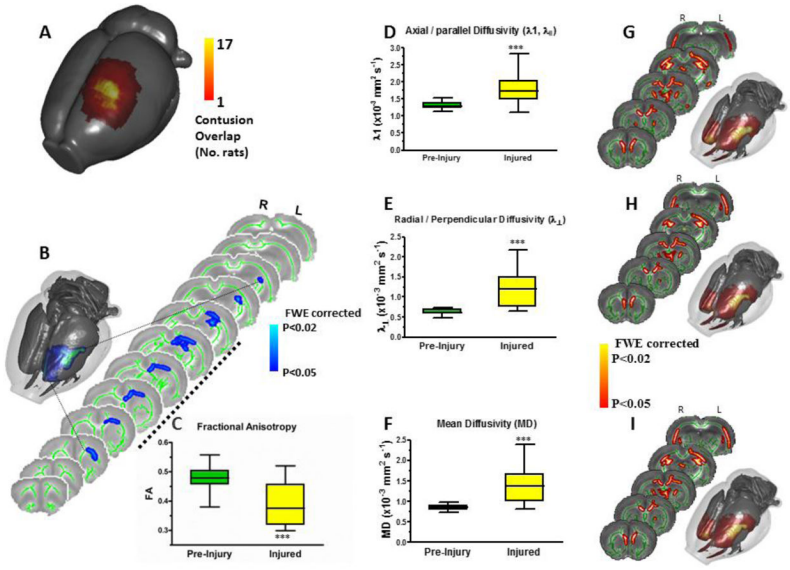

Fig. 3. CCI injury results in a persistent, unilateral reduction in FA at 28 days post-injury as well as increases in AD, RD and MD

[**A**] Cortical projection overlap map of contusion cavity volume for 17 rats at 28 days post-injury. The final contusion size from all brains was identified on T2-weighted images at 28 days post-injury and warped onto a 3D template brain. [**B**] Coronal and 3D rendered surface projection images showing significant, group-wise reductions in FA (blue regions) at 28 days especially in the primary contusion site (dotted line), when compared to pre-injury and controlling for contusion severity. Data obtained by TBSS analysis and superimposed on mean FA pre-injury images. [**C**] Average ROI FA data obtained from the significant region in [**B**] back-projected onto each rat confirmed the group reduction in FA. [**D**] AD, [**E**] RD, and [**F**] MD ROI data computed from the same region of reduced FA in [**B**] shows that all parameters are significantly increased from pre-injury in the same corpus callosum regions. White matter analysis of [**G**] AD, [**H**] RD, and [**I**] MD unconstrained by reductions in FA but controlling for injury severity revealed significant bilateral increases (red-yellow) in all parameters in corpus callosum and some subcortical regions that extended far beyond the significant reductions in FA. Data obtained by cluster-size-based statistical analysis ($z=1.7$, $P<0.05$, family-wise error (FWE) corrected, unpaired t test). Key: L- left, R- right; *** = $P<0.001$. Dotted line- primary region of contusion cavity.

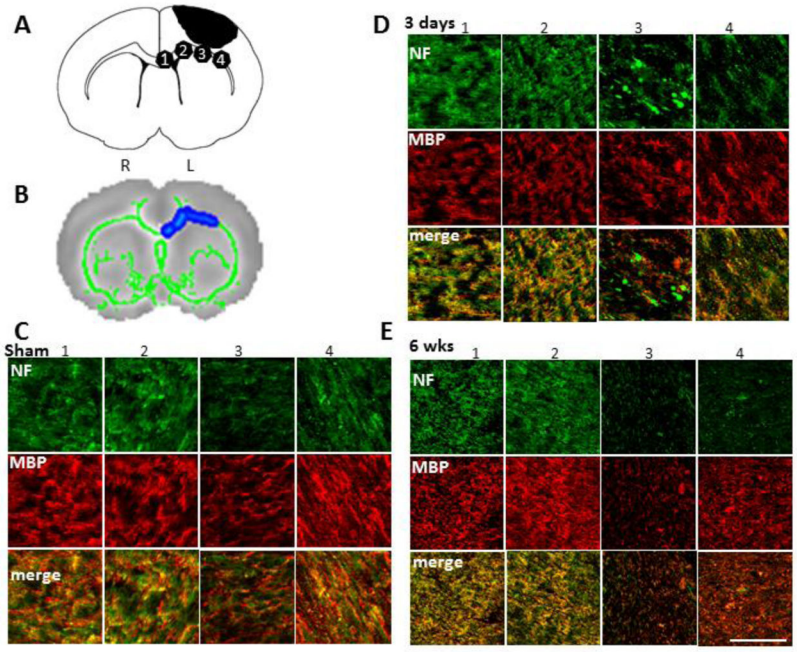

Fig. 4. Reduction in neurofilament staining and loss of myelin underlies reduction in corpus callosum FA

Coronal sections at the level of [**A**] the contusion cavity and [**B**] the region of reduced FA within the sensorimotor region were taken from [**C**] sham-control and injured rats at [**D**] 3 days, and [**E**] 6 weeks post-injury and immunostained for axonal neurofilament-160 (NF, green) and myelin basic protein (MBP, red). [**A**] Regions-of-interest (1– 4) along the corpus callosum in [**B**] the region of reduced FA show [**D**] disrupted axonal integrity indicated by punctate NF staining with dystrophic and bulbous ends, and reduced myelin content even by 3 days in regions 3 and 4 compared to [**C**] sham, with [**E**] significant loss of neurofilament structure and disordered myelin over an expanded are of white matter (regions 1–4) at 6 weeks. Scalebar=50um.

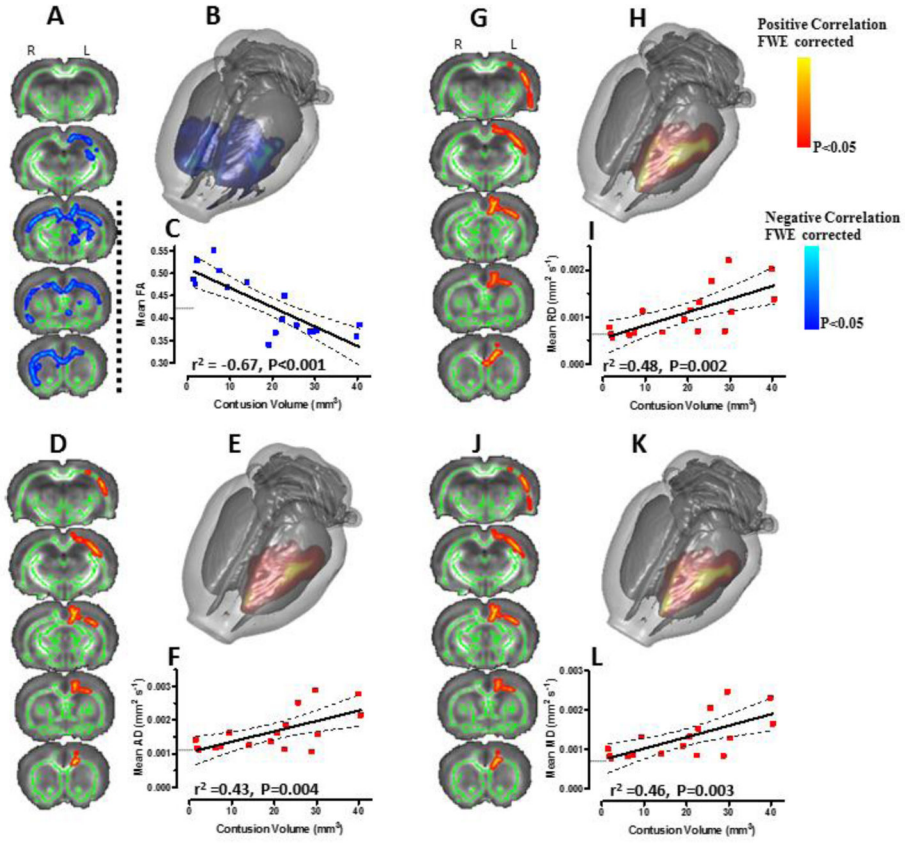

Fig. 5. Bilateral brain regions of reduced FA, but only unilateral regions of increased AD, RD and MD are associated with injury severity at 28 days after injury

TBSS correlation data using TBSS and contusion size as a covariate for [**A–C**] FA, [**D–F**] AD, [**G–I**] RD, and [**J–L**] MD at 28 days after injury. [**A**] Mean FA coronal sections and [**B**] a 3D volume white matter project image showing the white matter regions where reductions in FA within the injured group at 28 days were significantly and negatively associated with injury severity (blue regions). [**C**] Plot of region-of-interest FA values in each injured rat at 28 days obtained using the significant regions in [**A,B**] confirm the negative association between FA and injury severity at 28 days. Corresponding coronal images, 3D white matter projection images and individual brain ROI plots for [**D,E,F**] AD, [**G,H,I**] RD, and [**J,K,L**] MD indicating that unlike bilateral changes in FA, the underlying diffusion indices were all increased (red-yellow regions) and positively correlated to injury severity, but only within the ipsilateral white matter. Key: L- left, R- right. Dotted line- primary region of contusion cavity. Grey horizontal line in each graph is the mean pre-injury control value for the injury-significant region.

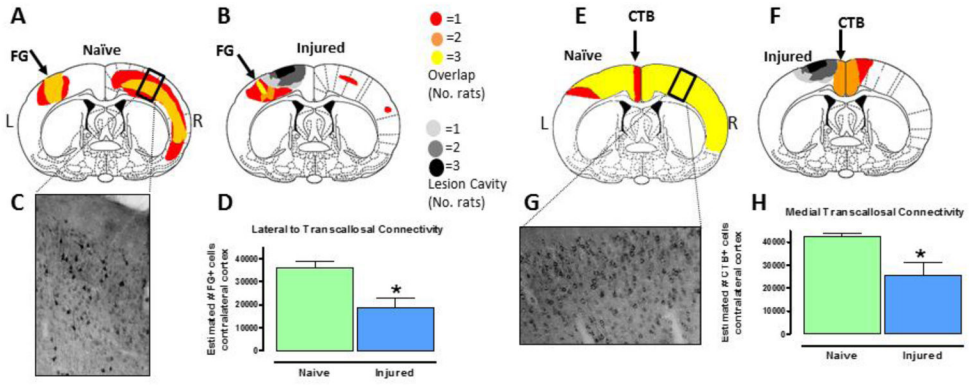

Fig. 6. Dye tract-tracing confirms loss of axonal integrity and reduced interhemispheric connectivity within the corpus callosum at 35 days after injury

The retrograde tract tracers Fluorogold (FG) and cholera toxin B (CTB) were injected in layer V of the cortex lateral to the contusion and medial to the contusion in 3 injured rats at 28 days and in three naïve controls, and labelled cells counts were made 7 days later. Extent of the cell labelling overlap between rats in sections immunostained for FG in [**A**] naïve and [**B**] injured rats, and for CTB in [**E**] naïve and [**F**] injured rats. Typical image of contralateral cortical cell labelling for [**C**] FG and [**G**] CTB. Quantitative plots of estimated number of [**D**] FG and [**H**] CTB labelled cells in the contralateral cortex indicating significant reduction due to injury. Key: *=P<0.05, L= left (ipsilateral hemisphere), R= right (contralateral hemisphere).

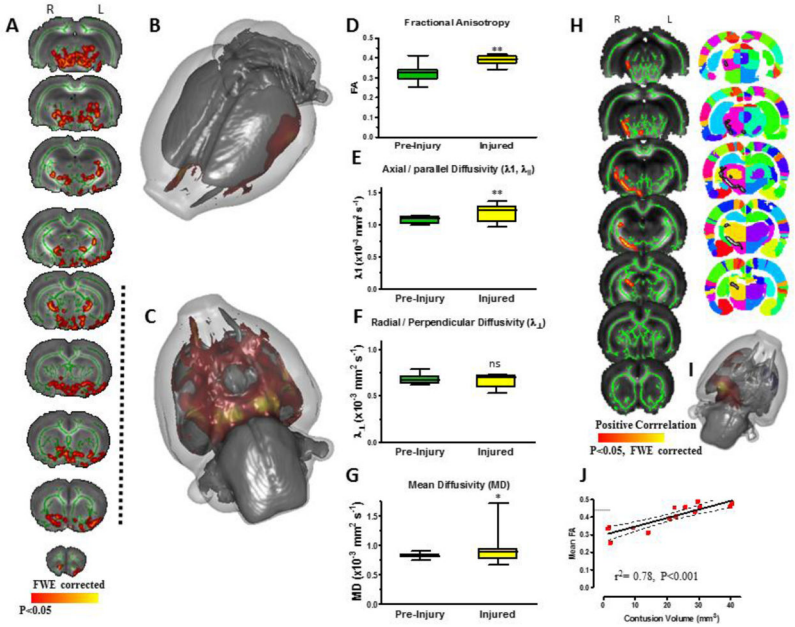

Fig. 7. Increases in FA occur in subcortical regions remote from areas of FA reduction, and are positively correlated to injury severity at 7 days post-injury.<

br>[**A**] Coronal images of group-wise, significant increases (red-yellow) in FA at 7 days post-injury compared to pre-injury and controlling for contusion severity at 28 days, superimposed on the axonal skeleton and mean FA maps identified through TBSS analysis (cluster-size-based statistical analysis, z=1.7, P<0.05, FWE) and [**B**] dorsal and [**C**] ventral views of the corresponding white matter surface projection maps. Plots of [**D**] mean FA within the significant region in [**A**] and the corresponding values of [**E**] AD, [**F**] RD and [**G**] MD indicating that increases in both AD and MD but not RD underlie the increased FA values. [**H**] Coronal brain and rat atlas images showing that the increase in FA within the contralateral internal capsule is positively correlated with injury severity (red region in brain, red/hot region in atlas, z=1.7, P<0.05, FWE). [**I**] 3D projection plot of [**H**]. [**J**] Plot of mean FA within the significant region in [**H**] for each brain at 7 days post-injury versus injury severity (contusion volume) showing a significant association. Key: L- left, R- right; ** = P<0.01, *=P<0.05, ns- not significant. Dotted line- primary region of contusion cavity. Grey horizontal line in [**J**] is the mean pre-injury control value for the injury-significant region.

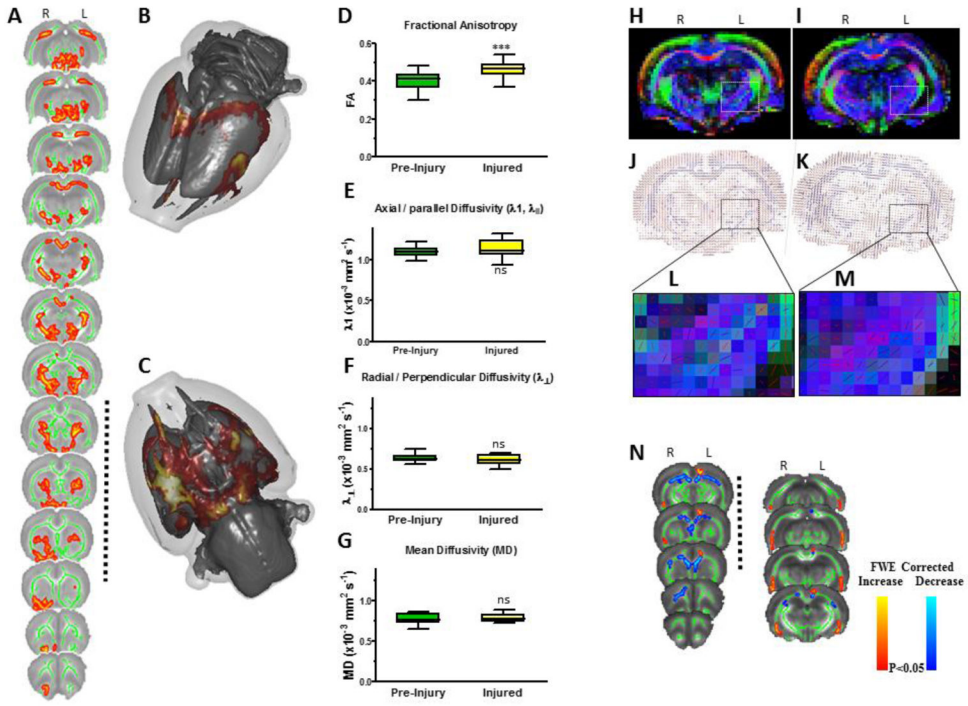

Fig. 8. Subcortical increases in FA persist at 28 days post-injury and are not associated with a reduction in crossing fibers.<

br>[**A**] Coronal images of group-wise, significant increases (red-yellow) in FA at 28 days post-injury compared to pre-injury and controlling for contusion severity, superimposed on the mean axonal skeleton and mean FA maps identified through TBSS analysis (cluster-size-based statistical analysis, z=1.7, P<0.05, FWE) and [**B**] dorsal and [**C**] ventral views of the corresponding white matter surface projection maps. Plots of [**D**] mean FA with in the significant region in [**A**] and the corresponding values of [**E**] AD, [**F**] RD and [**G**] MD, indicating that increases in FA are not accompanied by a change in any other DTI indices examined at 28 days post-injury. Representative coronal primary eigenvector images modulated by FA [**H, I, L,M**] from a rat [**H,L**] before injury and [**I**] 28 days after moderate injury fitted with a two-fiber diffusion model showing crossing fibers throughout the brain [**J, L**] before and [**K,M**] after injury (red/blue crossing lines) that is present in internal capsule before injury [**L, inset from H, J**] and after [**M, inset from I, K**]. [**N**] Regions of significant change in MO at 28 days compared to pre-injury showing that neither MO reductions (blue regions ~ tract disorganization) nor increases (red region ~greater tract complexity or number of crossing fibers) explain the increases in FA within subcortical regions. Key: L- left, R- right; *** = P<0.001, ns- not significant. Dotted line- primary region of contusion cavity.

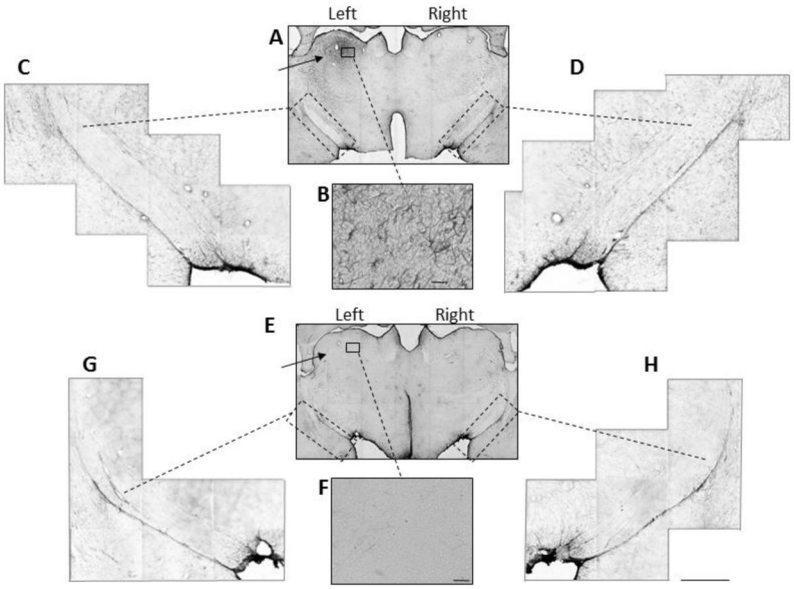

Fig. 9. Reactive astrocytes persist within dorsolateral thalamus but not in internal capsule at 4 weeks post-injury

Representative brightfield micrographs of GFAP-positive astrocyte immunohistochemistry from coronal sections of [**A–D**] an injured brain at 4 weeks post-injury and [**E–H**] a naïve brain. At low magnification [**A, E**] gliosis is found in dorsolateral thalamus of [**A**] injured brain (and **B**, boxed region at high magnification) and not present in the [**E**] uninjured brain and at higher magnification [**F**] (arrows). At higher magnification of the inset area (dotted line box, **A, E**) some reactive astrocytosis is visible at the base of brain within the internal capsule on both [**C**] ipsilateral and [**D**] contralateral sides of the injured brain, but very little in other areas, similar to the naïve brain [**G, H**]. Bar is 250μm [**C,D,G,H**) and 50μm (**B,F**).

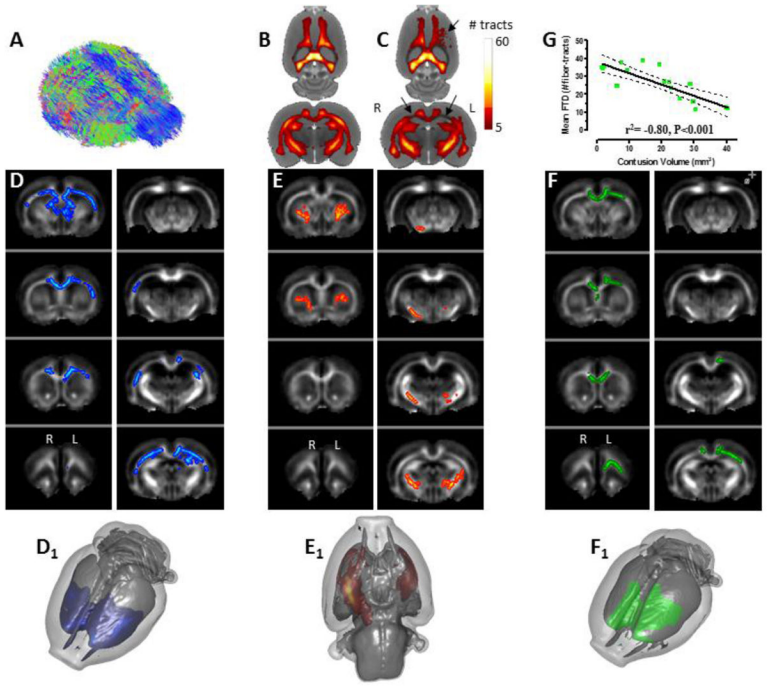

Fig. 10. Changes in fiber track density (FTD) are spatially consistent with changes in FA.< br>[**A**] Whole brain tractography was used to compute the number of fiber tracts/voxel and the group mean density showed gross decreases (arrows in [**C**] when comparing [**B**] pre-injury to [**C**] post-injury 28 day mean fiber tracts/voxel. [**D**] Coronal images of group-wise, decreases (blue) in FTD at 28 days post-injury compared to pre-injury and controlling for contusion severity, superimposed on the mean axonal skeleton and mean FA maps identified through TBSS analysis (cluster-size-based statistical analysis, z=1.7, P<0.05, FWE corrected) and [$\mathbf{D_1}$] rendered in 3D. [**E]** Increases in FTD (red-yellow) at 28 days post-injury compared to pre-injury and controlling for contusion severity (threshold free cluster enhancement, P<0.05, corrected) and [$\mathbf{E_1}$] rendered in 3D. [**F**] Regions where FTD is negatively correlated (in green) to injury severity (P<0.05, corrected) and [$\mathbf{F_1}$] rendered in 3D. [**G**] Plot of mean FTD within the highlighted region in [**F**] versus injury severity (contusion volume) showing a significant negative correlation. Key: L- left, R- right. Grey horizontal line in [**G**] is the mean pre-injury control value for the injury-significant region.